Electronic Supplementary Material (ESI) for Journal of Materials Chemistry A.

Highly Efficient Organic Solar Cell with Superior Deformability Enabled by Diluting Small Molecule Acceptor Content

Qinglian Zhu, Jingwei Xue, Heng Zhao, Baojun Lin, Zhaozhao Bi, Susanne Seibt, Ke Zhou, Wei Ma

SUPPLEMENTAL INFORMATION

Experiment section

Materials. PTQ10, D18 and m-BTP-PhC6 were purchased from Hyper. Inc. and were used as received without further purification. The patterned glass/ITO substrates were purchased from South China Science & Technology Co., Ltd.

Device Fabrication: The organic solar cells deposited on glass in this work were fabricated with a conventional structure of ITO/PEDOT:PSS/active layer/PDINO/Al. The patterned indium tin oxide (ITO) glass (sheet resistance = 15 Ω/sq) was continuously precleaned in the ultrasonic bath with de-ionized water, acetone and isopropanol. Then, ITO was exposed to UVO (20 min) to reform the surface. After that, PEDOT:PSS layer was spin-coated at 5500 rpm onto the ITO glass substrates as hole transporting layer with a thickness of 30 nm, followed by annealing at 150 °C for 15 min. The active layer solution was prepared in chloroform with PTQ10 or D18 concentration of 4 mg/mL. The weight ratio of donor to acceptor is varied with 1:1.2, 1.2:1.2, 1.5:1.2 and 1.7:1.2 for binary PTQ10:m-BTP-PhC6 systems. The weight ratio of donor to acceptor for binary D18:m-BTP-PhC6 is 1:1.2. The weight ratio of PTQ10 to m-BTP-PhC6 for ternary PTQ10:D18:m-BTP-PhC6 is fixed as 1:1.2 with 20%, 50% and 70% of D18 incorporation (relative to the weight of PTQ10). Before spin-coating the active layer, 0.75% chloronaphthalene (v/v) was added to the solutions of all solutions. Binary D18:m-BTP-PhC6 solution was spin coated on the top of PEDOT:PSS with spin speed of 1000 to maintain a thickness of 100 nm. Solutions of binary PTQ10:m-BTP-PhC6 with D/A ratio of 1:1.2, 1.2:1.2, 1.5:1.2 and 1.7:1.2 were spin coated with spin speed of 2000, 2000, 2500, and 2500 to deliver thickness of 100 nm. As for ternary systems, thickness of 100 nm for active layers could be obtain with spin speed of 3000, 3500, and 4000 for D/A ratio of 1.2:1.2, 1.5:1.2 and 1.7:1.2. The active layers were annealed at 100°C for 10 min and then PDINO was spin-coated at 3200 rpm onto the annealed active layers with a thickness of 10 nm. Finally, 100-nm-

thick Ag layer was then evaporated under the vacuum environment (ca. 10−5 Pa) to form the cathode electrode. The measured area of the active device was 4 mm^2.

Device Characterization

The J-V characteristics were measured in the N2 glovebox under AM 1.5 G (100 mW cm^{-2}) using an AAA solar simulator (SS-F5-3A, Enli Technology CO, Ltd.) calibrated with a standard photovoltaic cell equipped with a KG5 filter and a Keithley 2400 source meter unit. Rigid cells have devices area of 4 mm^2, defined by a metal mask with aperture aligned with the device area. The steady absorption spectra were acquired on a Shimadzu UV-3600 Plus Spectrophotometer. The contact angle was obtained by KRUSS DSA 100 with water and diiodomethane. Transmission electron microscopy (TEM) was performed using a JEM-F200 instrument at 200 kV accelerating voltage. AFM characterization was scanned by Veeco INNOVA Atomic Force Microscope using a tapping mode. PL spectrum was recorded by FLS980 spectrometer (Edinburgh Instruments, EI). The UV−vis absorption spectrum was measured by a Shimadzu UV-3600 Plus Spectrophotometer. The film thickness was measured by a surface profilometer (Dektak XT, Bruker).

Pseudo Free-standing Tensile Test

The samples were prepared through following steps. First, active layers were blade coated on 1cm × 3 cm glasses covered with water soluble PEDOT:PSS layer (≈60 nm) to form a bilayer composite film structure with a semiconducting film of 120 nm thick. Then, the films were etched into the dog-bone shape through an oxygen plasma etcher with a dog-bone shaped PDMS mask for 10 min. The bilayer film was slowly dipped into a deionized water bath to release and float the dog-bone photovoltaic films by dissolving the underlying water -soluble PEDOT:PSS layer. Tensile grips were slowly descended to adhere with films on water. The tensile test was performed by applying strains at 9×10^{-2} %/s to the film through a motorized linear stage equipped with a digital encoder while monitoring the force exerted on the film with a high-resolution load cell.

Grazing Incidence Wide-Angle X-ray Scattering (GIWAXS) Characterization

GIWAXS measurements were performed at SAXS/WAXS beamline, Australian Synchrotron ANSTO. Samples were prepared on Si substrates using identical blend solutions as those used in devices. The 15.2 keV X-ray beam was incident at a grazing angle of 0.08°-0.12°, selected to maximize the scattering intensity from the samples. The scattered x-rays were detected using a Dectris Pilatus 2M photon counting detector.

Resonant Soft X-ray Scattering (RSoXS)

RSoXS transmission measurements were performed at beamline 11.0.1.2 at the Advanced Light Source (ALS). Samples for R-SoXS measurements were prepared on a PSS modified Si substrate under the same conditions as those used for device fabrication, and then transferred by floating in water to a 1.5 mm × 1.5 mm, 100 nm thick Si3N4 membrane supported by a 5 mm × 5 mm, 200 μm thick Si frame (Norcada Inc.). 2-D scattering patterns were collected on an in-vacuum CCD camera (Princeton Instrument PI-MTE). The sample detector distance was calibrated from diffraction peaks of a triblock copolymer poly(isoprene-b-styrene-b-2-vinyl pyridine), which has a known spacing of 391 Å. The beam size at the sample is approximately 100 μm by 200 μm.

In-situ Ultraviolet-visible (UV-vis) Absorption Measurements

Ultraviolet-visible (UV-vis) absorption measurements were performed by the Filmetrics F20-EXR spectrometer using the transmission mode with the time resolution of 0.04 s. The spectrometer consists of light source and detector. The light source and detector are fixed above and below the substrate, respectively, and on the same vertical line. The film was blade coated onto the glass substrate. The detector collects the transmission spectra ranged from 400 to 1050 nm during coating. The UV-vis absorption spectra are calculated from the transmission spectra according to the equation $A_\lambda = -\log_{10}(T)$, where A_λ is the absorbance at a certain wavelength (λ) and T is the calculated transmittance. The light source and detector were turned on before coating the film, so time zero is the point when the first solution transmission spectrum

was collected by the detector. Before time zero, there is only noise in the transmission spectra.

Mobility Measurements

The mobilities were measured by using a space charge limited current (SCLC) model with the hole-only device of glass/ITO/PEDOT:PSS/active layer/MoO_X/Al and electron-only device of glass/ITO/ZnO/ active layer /PDINO/Al. Hole mobility and electron mobility were obtained by fitting the current density-voltage curves and calculated by the equation:

$$J = 9\varepsilon_0\varepsilon_r\mu(V_{appl} - V_{bi} - V_s)^2/8L^3$$

Where J is current density, ε_0 is the permittivity of free space, ε_r is the relative permittivity of the material (assumed to 3), μ is hole mobility or electron mobility, V_{appl} is applied voltage, V_{bi} is the buit-in voltage (0 V), V_s is the voltage drop from the substrate's series resistance (V_s=IR) and L is the thickness of active layer.

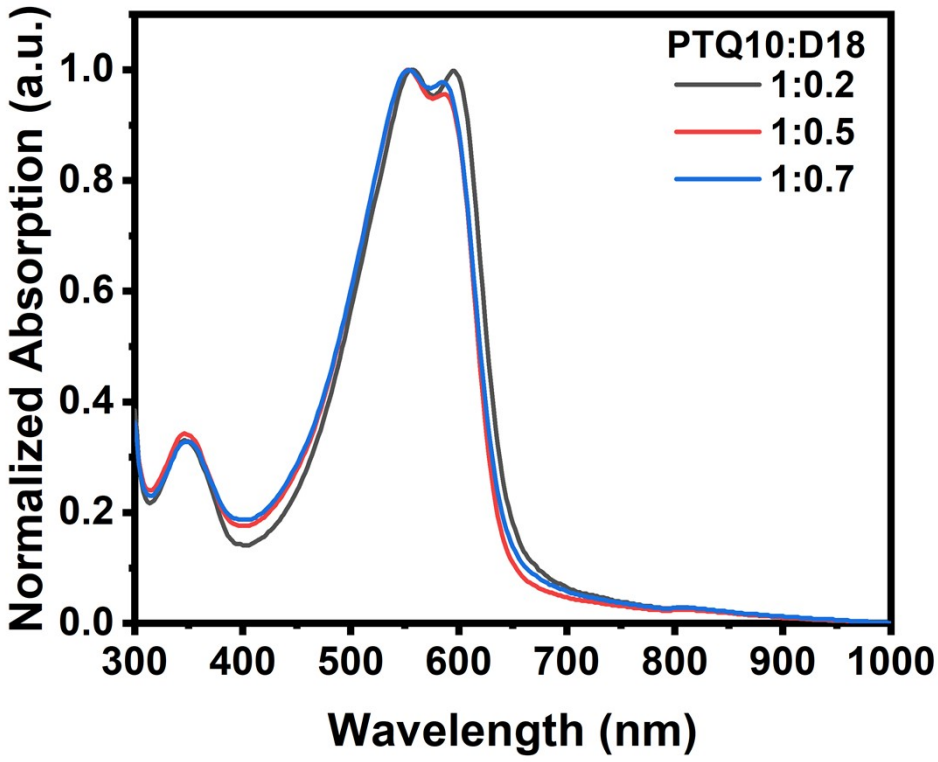

Figure S1. Normalized UV-vis absorption spectra of PTQ10:D18 films with ratio of 1:0.2, 1:0.5 and 1:0.7.

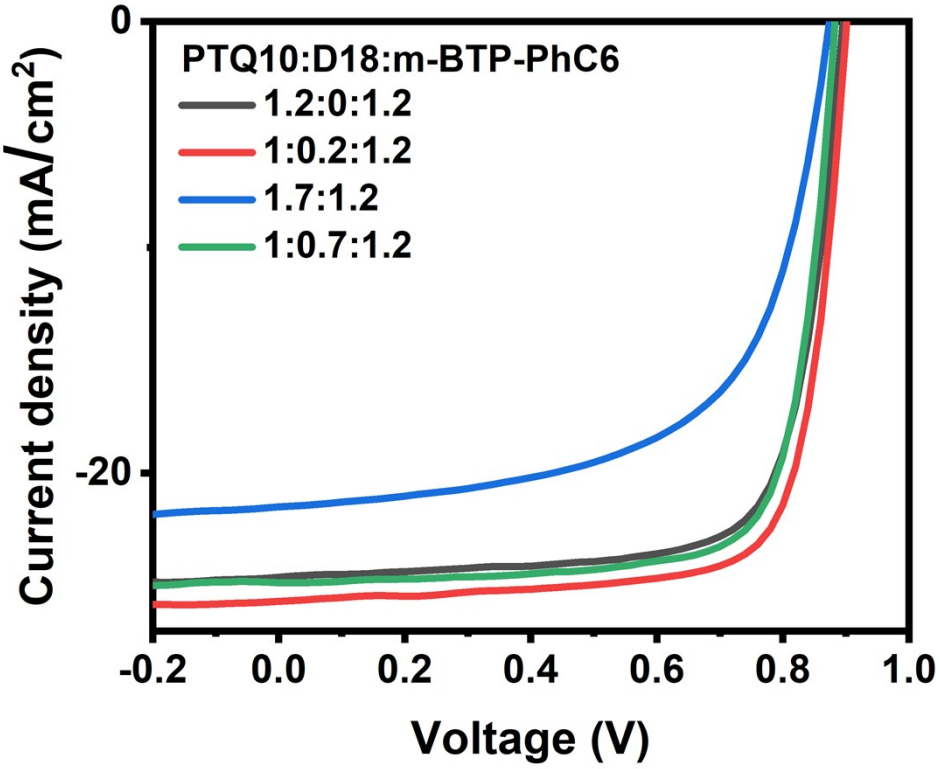

Figure S2. *J-V* curves of PTQ10:D18:m-BTP-PhC6 OSCs with various relative content of 1.2:0:1.2, 1:0.2:1.2, 1.7:0:1.2 and 1:0.7:1.2 under AM 1.5G, 100 mA/cm^2.

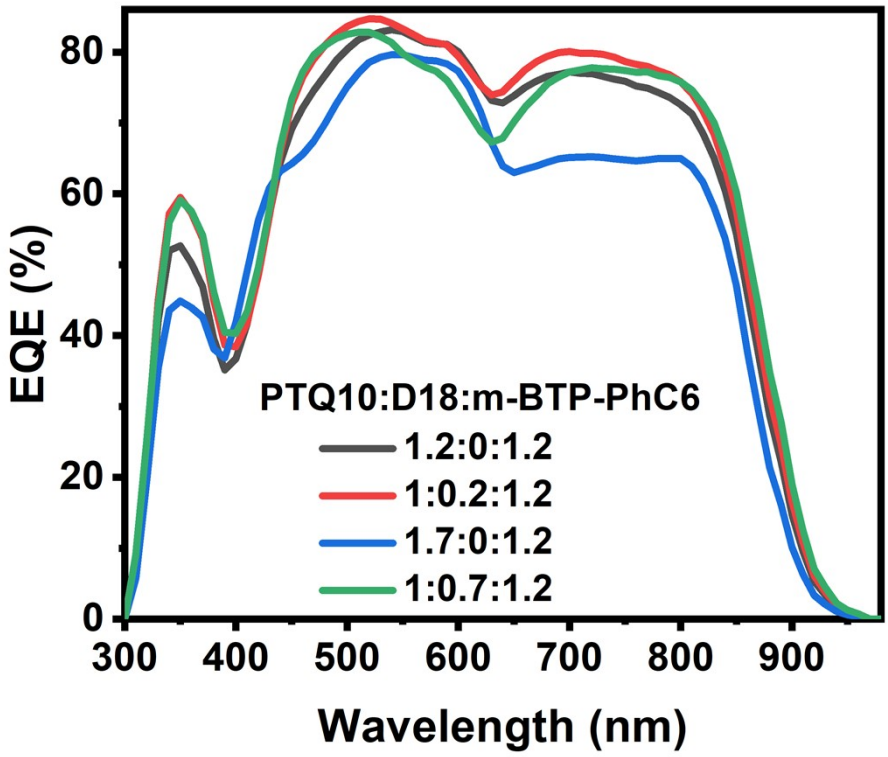

Figure S3. EQE curves of the 1.2:0:1.2, 1:0.2:1.2, 1.7:0:1.2 and 1:0.7:1.2.

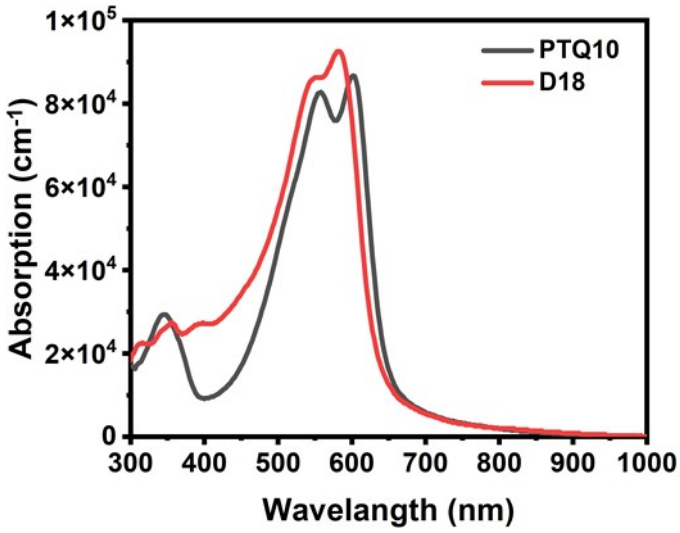

Figure S4. Absorption coefficients of PTQ10 and D18 films.

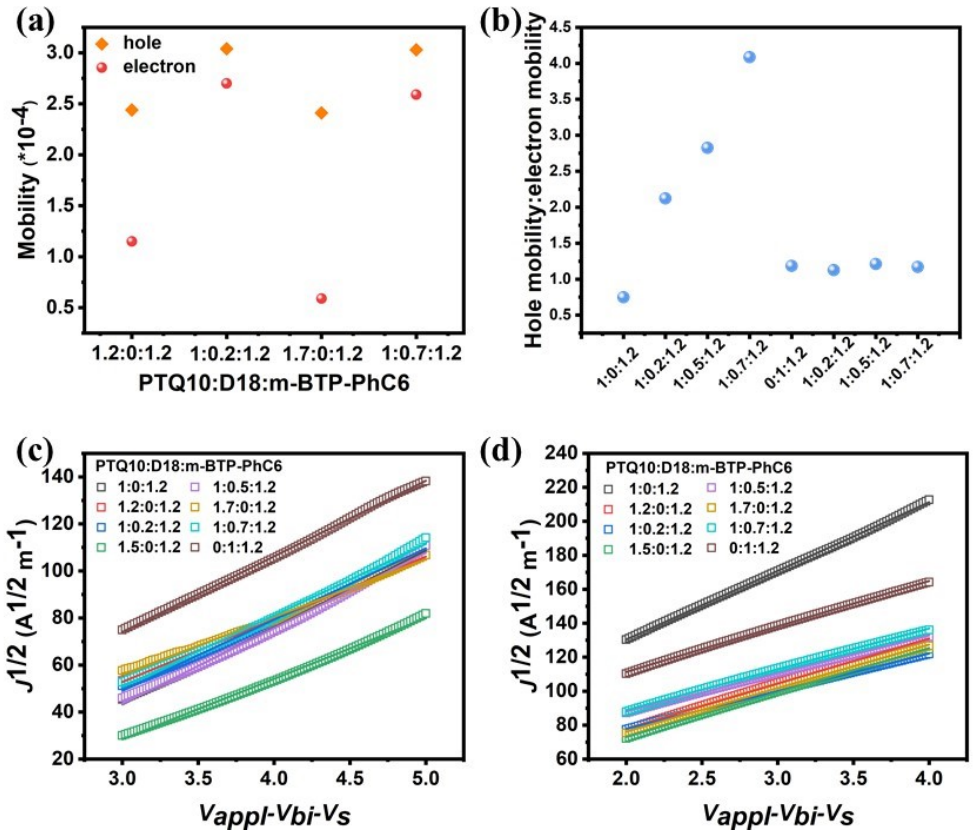

Figure S5. (a) Calculated mobility of PTQ10:D18:m-BTP-PhC6 OSCs with ratio of 1.2:0:1.2, 1:0.2:1.2, 1.7:0:1.2 and 1:0.7:1.2. (b) Value of hole:electron mobility as the function of PTQ10:D18:m-BTP-PhC6 with different relative ratio. $J^{1/2}$-V characteristics of (c) electron-only and (d) hole-only devices based on PTQ10:D18:m-BTP-PhC6 OSCs with ratio of 1.2:0:1.2, 1:0.2:1.2, 1.7:0:1.2, 1:0.7:1.2.

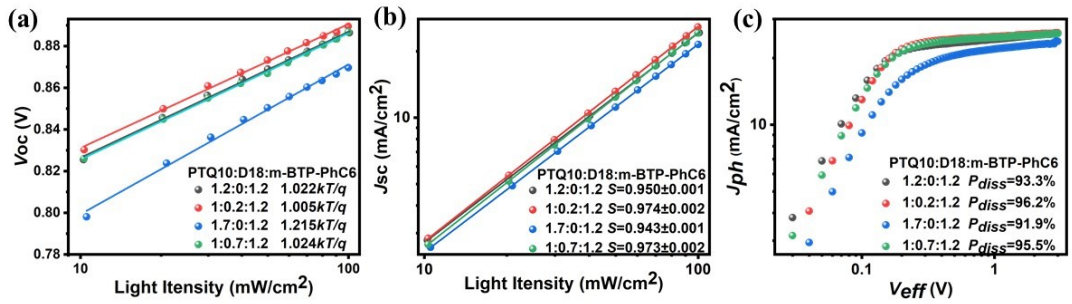

Figure S6. light intensity dependence of (d) V_{oc}, (e) J_{sc} and (f)J_{ph} versus V_{eff} plots of PTQ10:D18: m-BTP-PhC6 OSCs with ratio of 1.2:0:1.2, 1:0.2:1.2, 1.7:0:1.2, 1:0.7:1.2

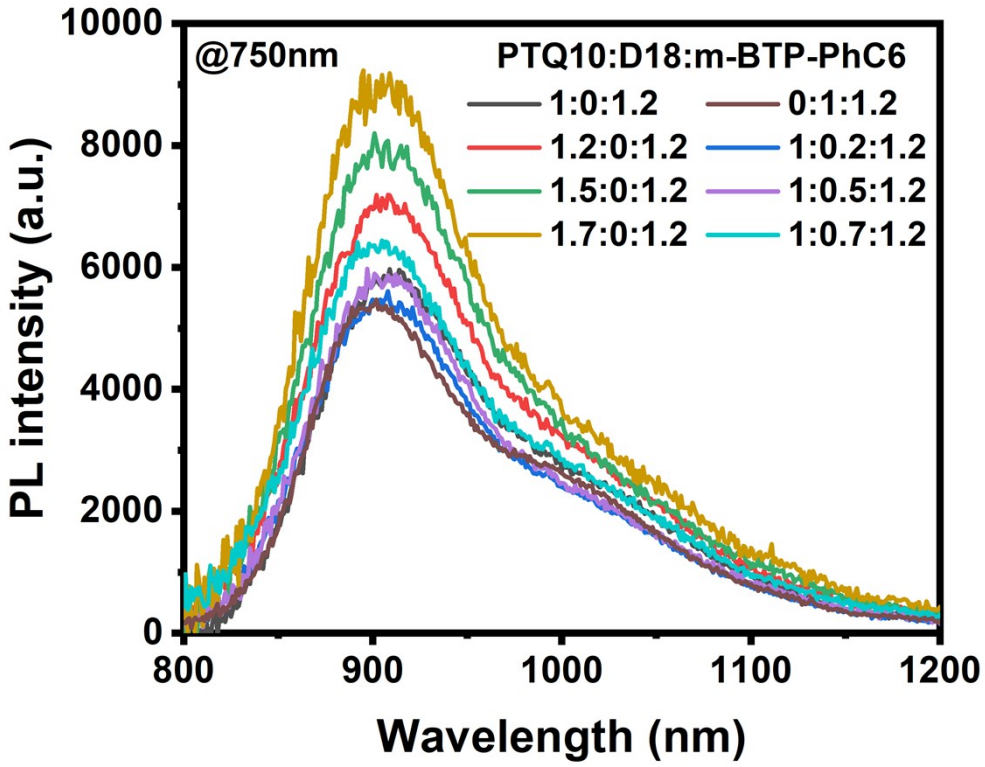

Figure S7. Photoluminescence spectra of PTQ10:D18: m-BTP-PhC6 films with different ratio.

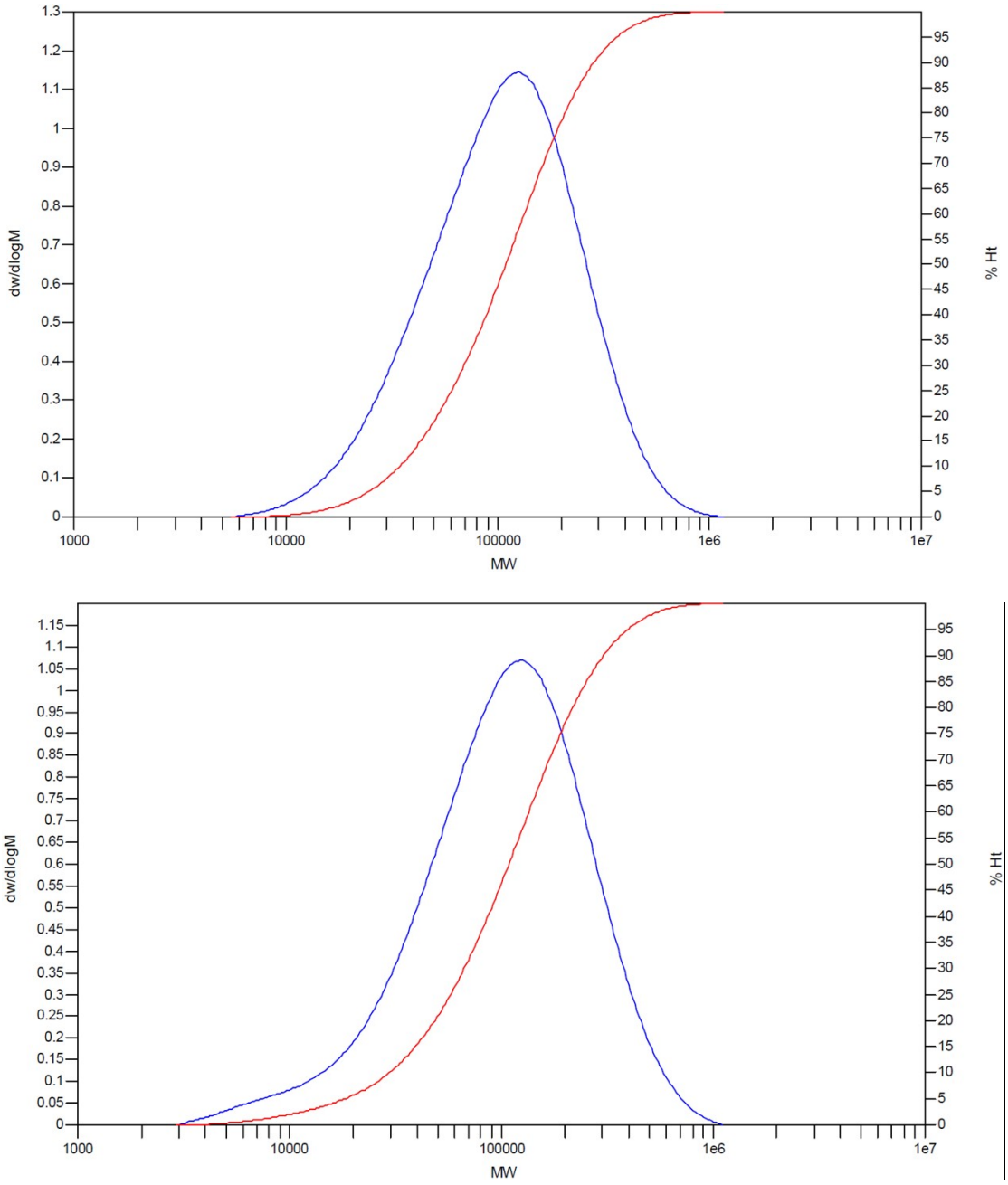

Figure S8. The molecular weight of D18 (top) and (b) PTQ10 (bottom) used in this manuscript.

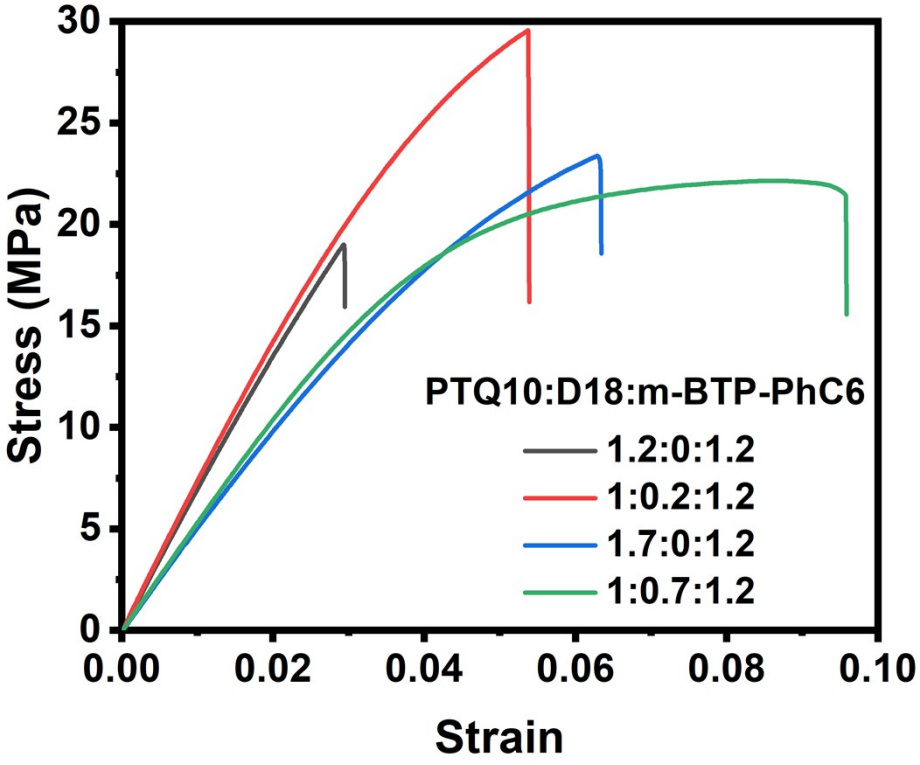

Figure S9. Stress-strain curves of PTQ10:D18:m-BTP-PhC6 films with ratio of 1.2:0:1.2, 1:0.2:1.2, 1.7:0:1.2, 1:0.7:1.2

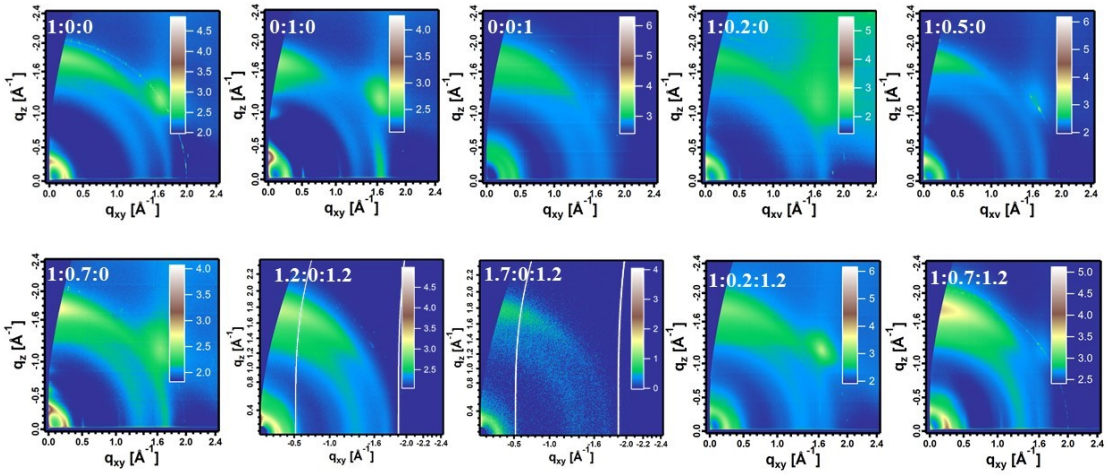

Figure S10. 2D GIWAXS patterns of PTQ10:D18: m-BTP-PhC6 films with different ratio.

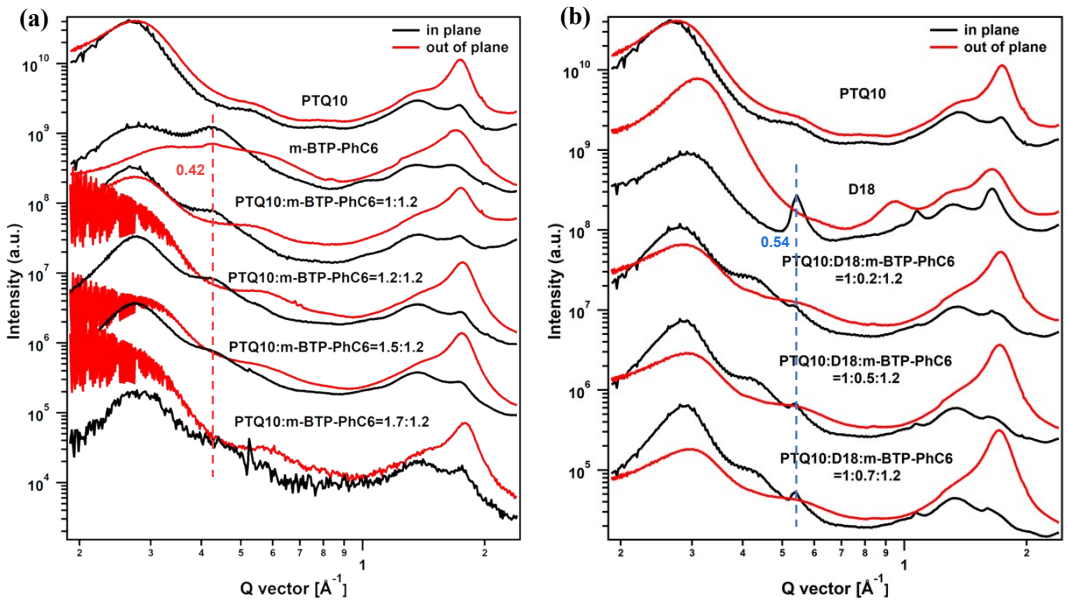

Figure S11. 1D GIWAXS profiles of PTQ10:D18: m-BTP-PhC6 films with different ratio.

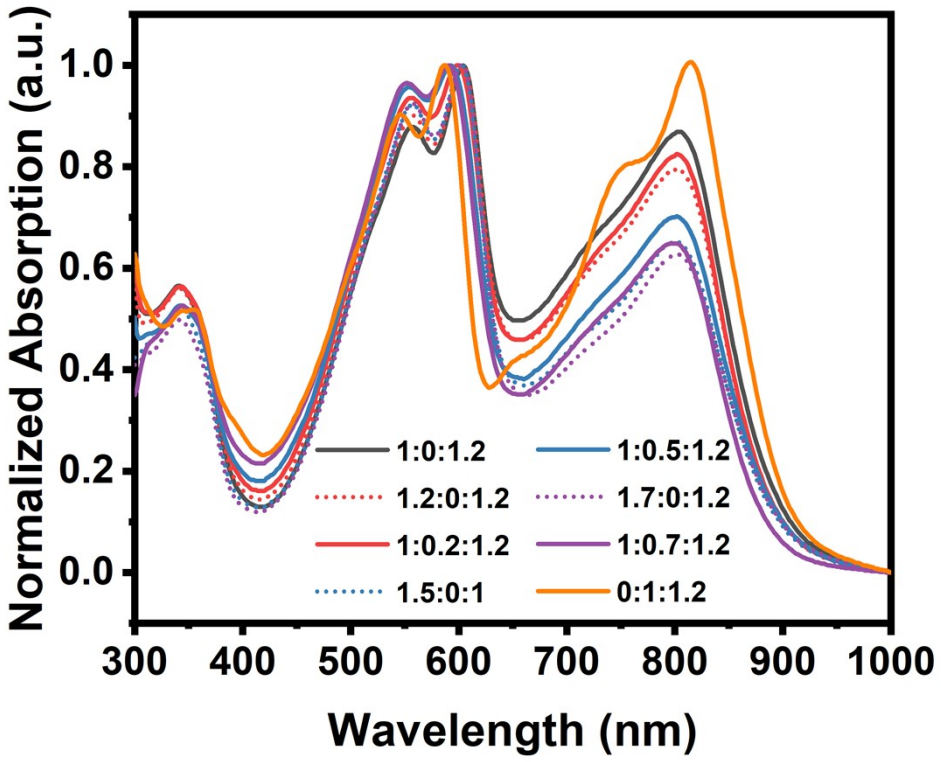

Figure S12. Normalized UV-vis absorption spectra of PTQ10:D18:m-BTP-PhC6 films with different ratios.

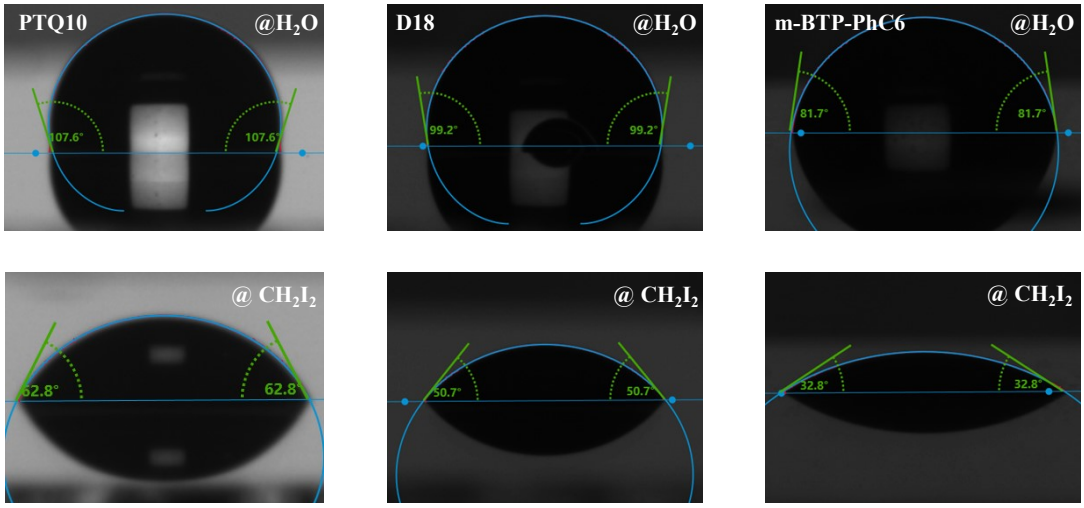

Figure S13. Contact angles of PTQ10, D18 and m-BTP-PhC6.

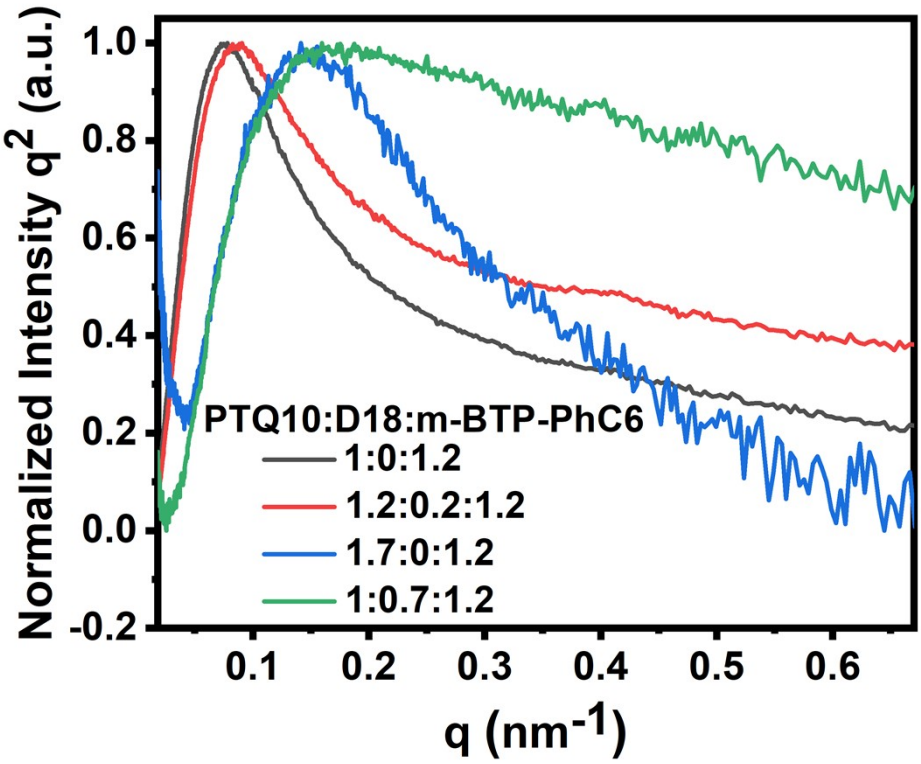

Figure S14. Normalized RSoXS profiles of PTQ10:D18:m-BTP-PhC6 films with ratio of 1.2:0:1.2, 1:0.2:1.2, 1.7:0:1.2, 1:0.7:1.2.

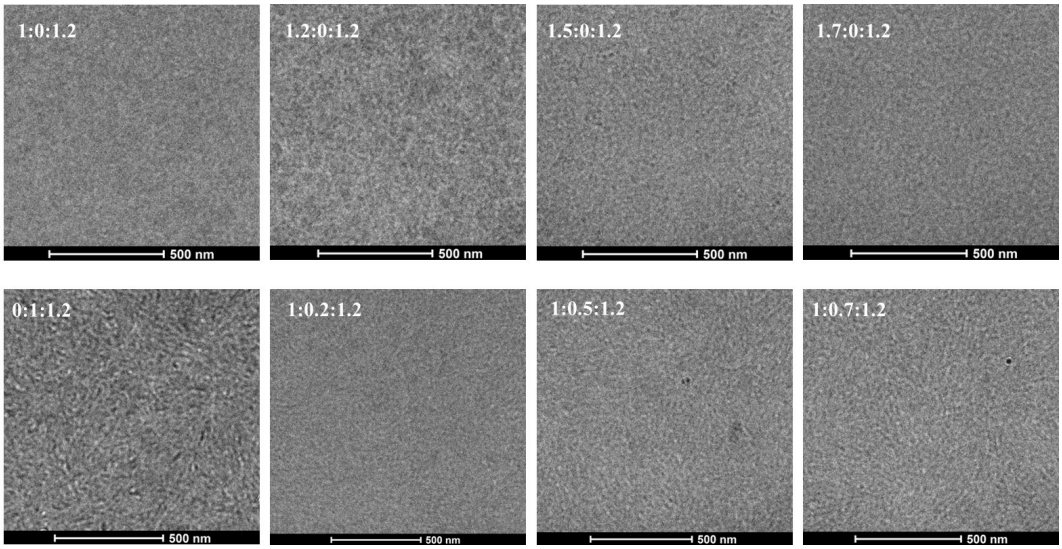

Figure S15. TEM images of PTQ10:D18:m-BTP-PhC6 films with different ratio.

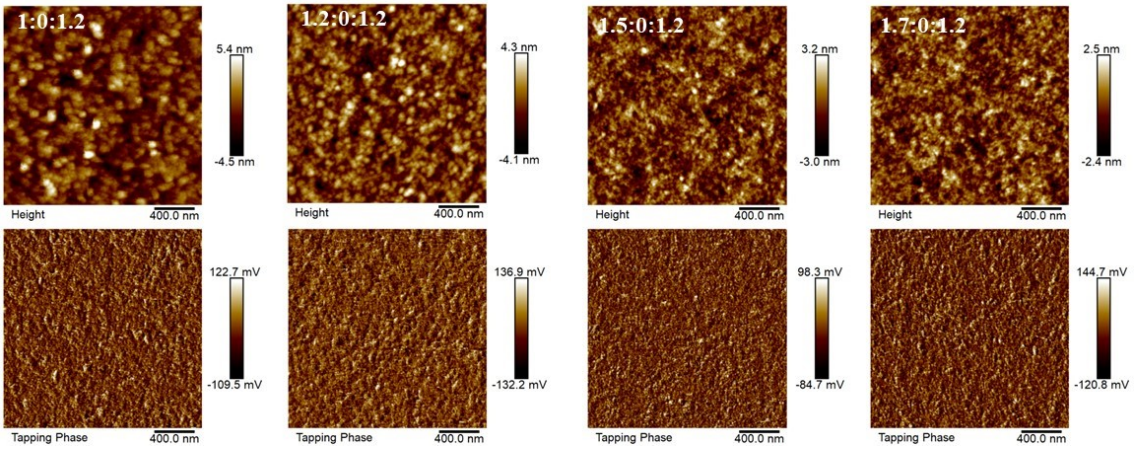

Figure S16. The height (top line) and phase (bottle line) AFM images of PTQ10:D18: m-BTP-PhC6 films with ratio of 1:0:1.2, 1.2:0:1.2, 1.5:0:1.2, 1.7:0:1.2.

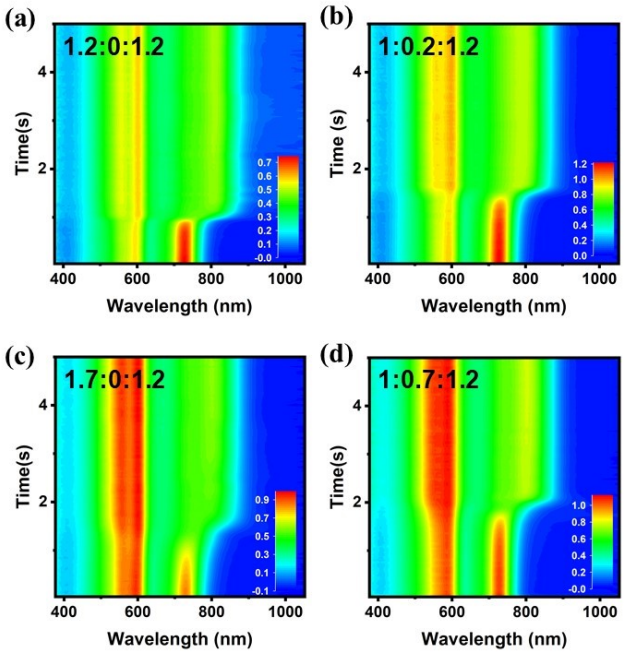

Figure S17. Time-dependent contour maps of UV-vis absorption spectra of PTQ10:D18:m-BTP-PhC6 films with ratio of (a) 1.2:0:1.2, (b) 1:0.2:1.2, (c) 1.7:0:1.2, (d) 1:0.7:1.2.

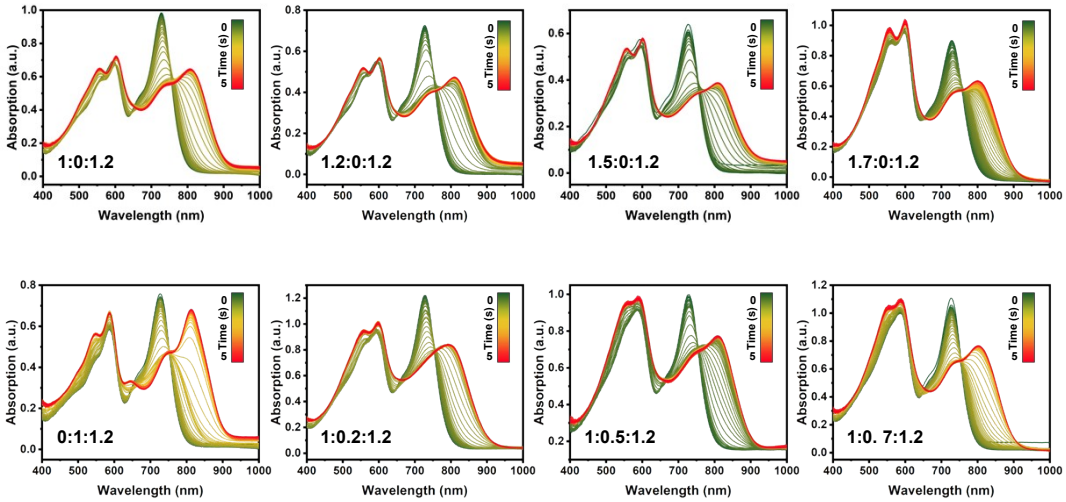

Figure S18. In-situ UV-vis absorption spectra of PTQ10:D18:m-BTP-PhC6 films with different ratio.

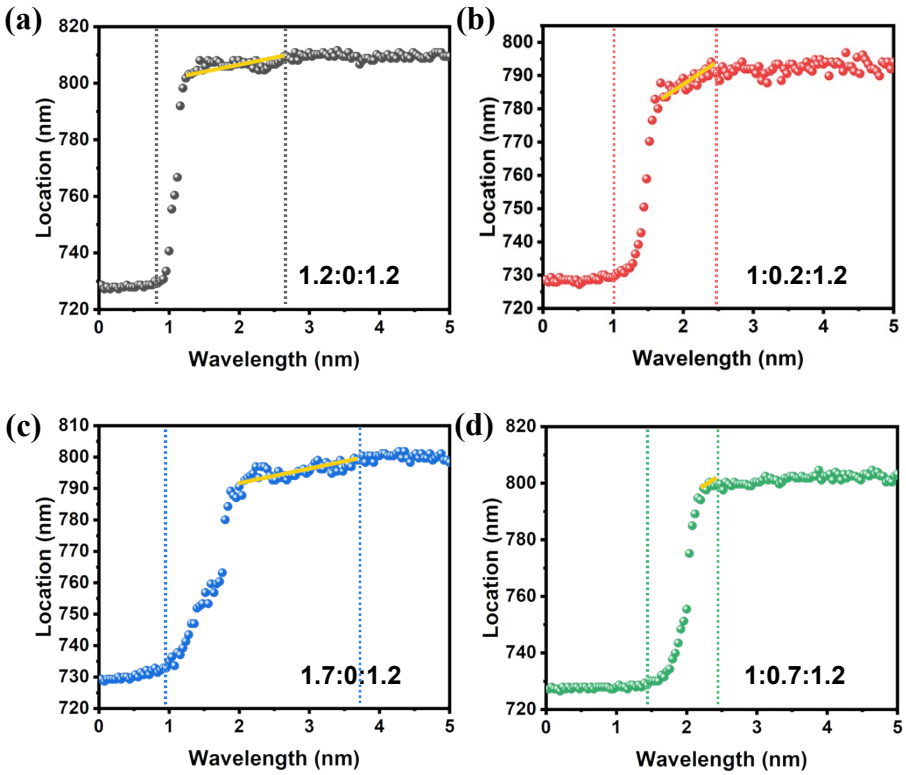

Figure S19. Time evolution of peak location of m-BTP-PhC6 of PTQ10:D18:m-BTP-PhC6 films with ratio of (a) 1.2:0:1.2, (b) 1:0.2:1.2, (c) 1.7:0:1.2, (d) 1:0.7:1.2.

Table S1. Summary of photovoltaic parameters of PTQ10:D18:m-BTP-PhC6 OSCs

with ratio of 1.2:0:1.2, 1:0.2:1.2, 1.7:0:1.2, 1:0.7:1.2 under AM 1.5G, 100 mA/cm^2.

PTQ10:D18:m-BTP-PhC6	V_{oc} (V)	J_{sc} (mA/cm^2)	FF (%)	Efficiency (%)
1.2:0:1.2	0.893±0.003	24.3±0.3	74.1±0.8	16.1±0.2
	0.896	24.6	74.2	16.3
1:0.2:1.2	0.892±0.006	25.7±0.2	75.5±0.6	17.3±0.2
	0.901	25.7	76.0	17.6
1.7:0:1.2	0.878±0.003	21.3±0.5	60.4±1.0	11.3±0.2
	0.874	21.5	61.3	11.5
1:0.7:1.2	0.891±0.006	24.8±0.2	74.3±1.1	16.5±0.2
	0.883	24.8	76.0	16.7

Table S2. The summarized surface free energy, solubility parameters, and interaction parameters.

i	γ_s [mN/m]	δ [MPa$^{1/2}$]	χ [D18, i]
D18	34.09	21.42	
PTQ10	26.97	19.05	0.522
m-BTP-PhC6	45.42	24.72	0.694

Table S3. The Phase Separation Parameters of PTQ10:D18:m-BTP-PhC6 blend films with ratio of 1.2:0:1.2, 1:0.2:1.2, 1.7:0:1.2, 1:0.7:1.2.

PTQ10:D18:m-BTP-PhC6	Location (nm^{-1})	Domain size (nm)
1.2:0:1.2	0.0778	40.4
1:0.2:1.2	0.0883	35.6
1.7:0:1.2	0.145	21.6
1:0.7:1.2	0.150	20.9

Table S4. Mechanical property of the active layers and related device performance of

representative binary OSCs based on polymer:small molecule systems reported in literatures and this work.

Donor:acceptor	PCE (%)	COS (%)	Ref.[a]
P3HT:PC61BM	0.6	3.0	40
PCE10:FOIC(BHJ)	11.0	3.1	41
PCE10:FOIC(P-i-N)	11.4	18.5	41
PCE10:N2200	5.9	11.6	27
PCE10:N2200:$PC_{71}BM$(30%)	10.7	6.8	27
PM6:IDIC16	4.93	1.4	20
PM6:Y6	15.4	5.8	42
PM6:Y7	14.8	2.3	31
PM6-C5:Y7	16.2	12.1	31
PM6-C10:Y7	16.7	9.2	31
PM6-C20:Y7	14.7	6.1	31
PM6-C30:Y7	13.6	3.8	31
PCE10:PC71BM	6	1.1	43
PCE10:ITIC	6.4	3.4	43
PBDB-T:Y5-2BO	7.0	2.3	21
PTQ10:D18:m-BTP-PhC6(1:0.2:1.2)	17.6	5.4	This work
PTQ10:D18:m-BTP-PhC6(1:0.5:1.2)	17.3	8.8	This work
PTQ10:D18:m-BTP-PhC6(1:0.7:1.2)	16.7	9.6	This work

[a]: Ref. number listed here corresponds to the number shown in Fig. 3e in the manuscript and detailed reference information is also recorded in the manuscript.